Modeling the behavior of deformable elastic matrix with damage model using particulate method (SPH)

DEPTULSKI Rafael C.[a*], DYMITROWSKA Magdalena[a], KONDO Djimédo [b]

a. PSE-ENV/SEDRE/LETIS, Institut de Radioprotection et de Sûreté Nucléaire (IRSN), 31 Avenue de la Division Leclerc, 92260 Fontenay-aux-Roses.
*Corresponding author: rafael.chavesdeptulski@irsn.fr
b. Sorbonne Université, Institut Jean le Rond d'Alembert - UMR 7190, 4 Place Jussieu, 75005 Paris

Abstract :

The hydromechanical behavior of saturated and partially saturated clay rocks has experienced in last decades an increase of interest due to potential applications (radioactive wastes disposal, CO2 storage). One of the critical issues is related to the assessment of initiation and evolution of fractures, both at macroscopic and pore scales. Despite the efforts to numerically capture such phenomena, several questions are still open, for instance, related to the capability of models to predict fracture localization. The present paper aims to assess the use of a Lagrangian particulate approach, based on the SPH (Smoothed Particles Hydrodynamics) method, which can address in the same formalism two-phase flow, movement of rigid inclusions and damage evolution in an elastic phase. In order to test the capability of SPH to describe the elastic damageable behavior, simulations of a bar submitted to a dynamical tensile load were conducted. Furthermore, we implemented and tested different energy-based formulations of damage models. The obtained results demonstrate that the SPH method can capture both damage evolution and localization in dynamic conditions. It shows that the size of the damaged zone is independent of the particle density (equivalent to the mesh size in a finite elements approach) in SPH and only dependent on the size of the smoothing/averaging neighborhood. This methodological study will be helpful to guide the application of the SPH method to entirely or partially saturated natural rocks.

Keywords: Rock fracture, elastic damage model, size-dependent constitutive model, Smoothed Particle Hydrodynamics.

1 Introduction

Indurated clays are among the rocks examined for radioactive waste disposal projects. In contempt of voluminous research carried out in recent decades, their hydromechanical behavior is not yet fully understood at the pore scale given that the difficulty to observe at nano-scale the initiation of macroscopic fractures and to recreate the conditions existing in situ. Marschall *et al.* [1] have introduced the phenomenological gas transport mechanisms in deep argillaceous formations, where the transport of gas through a very low-permeability clayey rock is controlled by hydro-mechanical properties and state (*i.e.* water saturation, porewater pressure, stress state) as well as by the gas pressure. Experimental evidence

[2] indicates that the gas percolation through saturated pores of clays intervenes by preferential pathways (which are highly unstable and partially reversible), accompanied by an expansion of the entire samples. Thus, in a water-saturated host rock, the classical visco-capillary flow (usually considered and well understood) may not be a suitable description of gas migration. Furthermore, dilatant flows are still poorly characterized both from experimental and theoretical perspectives. In the current work, we epitomize a model that can be useful to analyze such coupled phenomena at the pore scale, where the microstructure of the clay rock is explicitly represented by pores, clay matrix and rigid inclusions (quartz, carbonates, etc.). The clay matrix will be assumed to be an elastic material with damageable properties. In order to understand the properties of such a material and to evaluate the possibilities of simulating it, we first apply different models to the test case of a strain-softening bar under tensile forces. Bažant and Belytschko [3] were the first ones to propose an analytical solution to this dynamic problem taking into account the strain-softening behaviour of an elastic material. A few years later, Bažant postulated that the variable representing the damage to the material should be non-local. This proposition was based firstly on the strain-softening dependency on the microstructure scale [4, 5] and secondly on the fact that the locality would induce an ill-posed mathematical problem causing a mesh sensitivity of the solution. On the other hand, the non-local behavior is an inherent component of the Smoothed Particles Hydrodynamics and can correct such mathematical issues. For example, Vignjevic *et al.* [6] compared the Total Lagrangian form of SPH and the Finite Element Method highlighting the absence of mesh dependency in the solutions of the first one.

Following a normalized-corrected form of the standard SPH formulation [1], this work implements different energy-based local damage models, in order to discuss its pros and cons when compared to local methods and Total Lagrangian SPH. We will show that, in dynamic conditions, the proposed formulation can capture damage localization. Furthermore, it will demonstrate that the size of the damaged zone is independent of the particle density (no-mesh size dependence) and relate to a numerical parameter involved in the SPH method.

2 Methodology

2.1 Physical-model: Strain-softening bar configuration

For the sake of completeness, we recall here the 1D problem of a bi-tractioned bar (Fig. 1).

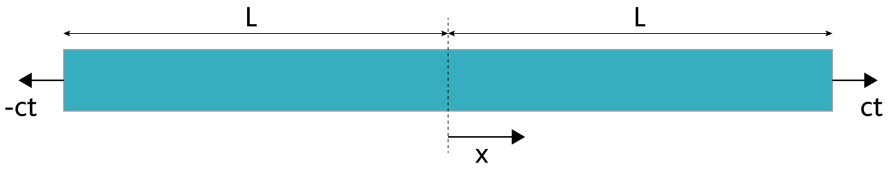

Figure 1: Bar configuration and boundary limits

Where c is the traction velocity, and ΔL is the displacement of each bar end after a time t. In this problem, the damage localization is expected at the center of the bar at the time $t = {}^{L}/_{v}$ where v is the sound wave speed. Three different bar configurations are proposed here, following [6]: 101, 151 and 201 particles along the longitudinal axis and, respectively, 5, 9 and 11 particles along its orthogonal axes. If the bar can be regarded as a continuum medium, the different particle densities can be regarded as different mesh refinements.

2.2 Numerical model: Smoothing Particles Hydrodynamics

SPH is a meshless method which was initially introduced by Gingold and Monaghan [7] and Lucy [8] for the treatment of astrophysical problems, and it is nowadays widely applied to simulate transient dynamic processes with significant deformations of the studied domain. Over the past decades, this model has been widely used in broader areas: On fluid dynamics, different applications for fluid flow [9, 10] and multiphase flows [11, 12] are acknowledged. Therefore, solid applications have been explored since the 1990s after the structural mechanics framework introduced by Libersky and Petscheck [13, 14]. Furthermore, applications in the field of heat transfer have also been proposed [15].

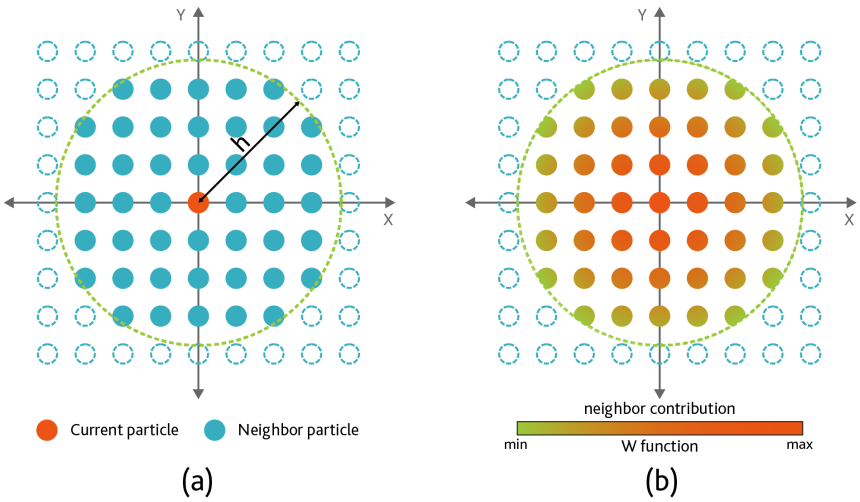

Figure 2: 2D SPH particles: (a) with smoothed length h; (b) with neighbor contribution weight following a smoothing function W

The method can be described as a Lagrangian particle method that does not use a structured grid. In SPH, an overall behavior is given as a result of the interpolation of the total particles contributions present in an elementary area, without their inter-connectivity. The constitutive laws are discretized in such domain using a smoothing function (also called kernel interpolation), in order to delimit the particle influence zone by a given smoothing length h (Fig. 2 - a). Therefore, the value of a field at each particle is approximated by a weighted sum of the field values at the neighboring particles (Fig. 2 - b). Following [16], the SPH method works by approximating a given f function using continuous integration and the Dirac's delta function $\delta(x)$.

$$f(x) = \int f(x')\delta(x - x')\mathrm{d}x' \tag{1}$$

The Dirac's delta is replaced by a smoothed function W in order to compute values of f utilizing the interpolation over neighboring values:

$$f(x) = \int f(x')W(x - x', h)\mathrm{d}x' + err_{smoothing} \tag{2}$$

Where h is the smoothing length, and $err_{smoothing} = \mathcal{O}(h^2)$ is the approximation error value [16]. Some conditions have to be respected by a smoothing function: it must converge to the Dirac's function when h tends to zero, it has a compact support of $2h$ as well as its integral is normalized to 1 on the whole domain. W must be an even function in order to achieve the same contribution from particles

located at the same distance. Furthermore, the fact to be positively defined inside the support domain has a physical meaning. Similarly, the smoothed derivatives of f can be obtained by the divergence theorem and integration by parts applied as presented in [16]:

$$\nabla \cdot f(x) = \int f(x') \cdot \nabla W_x(x - x', h) \mathrm{d}x' + err_{smoothing} \tag{3}$$

Some well-known smoothing functions have been designed to present high accuracy and numerical stability in different scenarios, whereas the Gaussian function conferred by Gingold [7] is a good option to achieve accuracy and stability but with a high computation cost. Thus, for computational convenience, smoothing functions are often expressed as polynomials forms, where among the most common formulations are the quadratic and cubic spline [16] which are frequently employed in hydrodynamics frameworks. Hence, the following cubic spline is the smoothing function adopted in the current work [17]:

$$W(x - x', h) = \frac{16}{\pi h^3} \begin{cases} \frac{1}{2} - 3r^2 + 3r^3 & \text{if } 0 \leq r < 0.5 \\ (1 - r)^3 & \text{if } 0.5 \leq r < 1 \\ 0 & \text{if } r \geq 1 \end{cases} \tag{4}$$

With $r = \frac{\|x - x'\|}{h}$ and $W(x - x', h)$ has unit of inverse the of volume. In a discrete model, the value for each particle is computed utilizing an interpolated weighted sum of contributions from its whole neighborhood (limited to h radius). The volume of each particle can be defined as:

$$V_i = \frac{m_i}{\rho_i} \tag{5}$$

Where i is the particle index. Hence, the continuous integrals presented in Eq. (2), moreover (3) can be approximated by their discrete forms:

$$f(x_i) = f_i = \sum_j f_j \, V_j \, W(x_i - x_j, h) = \sum_j f_j \, \frac{m_j}{\rho_j} \, W(x_i - x_j, h) \tag{6}$$

$$\nabla f_i = \sum_j (f_j - f_i) \frac{m_j}{\rho_j} \nabla W_{x_i}(x_i - x_j, h) \tag{7}$$

The summation over j covers all neighboring particles. Despite several advantages, using SPH requires solving some specific drawbacks. Thus, in this work, we have applied some model improvements: XSPH was introduced to improve the stability of simulation by correcting the non-physical noisy fluctuations of the particle velocities [18, 19]. Normalization of the shape W function and correction of its derivative ∇W were implemented in order to improve the accuracy of material properties, as shown in [18].

2.3 Elements of the elastic damage modeling

In a continuum damage mechanics approach, the macroscopic degradation process of a Representative Elementary Volume can be represented by a damage parameter D varying from 0 for sound to 1 for fully damaged material. The clay rock has been showing to exhibit a linear elastic behavior [20, 21] for a limited load range, beyond which appears damage behavior that can be coupled to elasticity or elastoplasticity [22]. Thus, we will consider that the clay material has elastic damageable behavior. In order to study such damage, we use the energy approach, as introduced by [23, 24]. For isotropic and nonviscous solid elastic damage material, the thermodynamic potential ω, the reversible Cauchy stress

σ and the damage energy release $\mathcal{Y}$ are given by:

$$\rho\omega\Big(\varepsilon,\mathrm{D}\Big)_i = \frac{1}{2}\mathrm{E(D)}_i\,\varepsilon_i^2 = \frac{1}{2}\sum_j \frac{m_j}{\rho_j}\,\mathrm{E(D)}_j\cdot\varepsilon_j^2\cdot W(x_i-x_j,h) \tag{8a}$$

$$\sigma_i = \rho\frac{\partial\omega_i}{\partial\varepsilon_i} = \mathrm{E(D)}_i\,\varepsilon_i = \sum_j \frac{m_j}{\rho_j}\,\mathrm{E(D)}_j\cdot\varepsilon_j\cdot W(x_i-x_j,h) \tag{8b}$$

$$\mathcal{Y}_i = -\rho\frac{\partial\omega_i}{\partial\mathrm{D}_i} = -\frac{1}{2}\mathrm{E'(D)}_i\cdot\varepsilon_i^2 = -\frac{1}{2}\sum_j \frac{m_j}{\rho_j}\,\mathrm{E'(D)}_j\cdot\varepsilon_j^2\cdot W(x_i-x_j,h) \tag{8c}$$

In which E is the Young material modulus and ε is the strain rate. Also, the superscript $'$ designates a function derivative. In a 1D configuration, the damage parameter D influences the elastic modulus of the material, $\mathrm{E(D)}$. Furthermore, based on the work of Ponte-Castaneda and Willis (PCW) [25] (see also [26] for further use in the context of damage mechanics), we adopted for the damage model (of microcracking) the following general form:

$$\mathrm{E(D)}/\mathrm{E}_0 = \frac{1-\alpha\mathrm{D}}{1+\beta\mathrm{D}} \tag{9}$$

Where the subscript $_0$ relates to an undamaged material, α and β being constant parameters allowing to define the damage function $\mathrm{E(D)}$. The damage energy release becomes in a general form:

$$\mathcal{Y}(\mathrm{D},\varepsilon) = \frac{(\alpha+\beta)}{2(1+\beta\mathrm{D})^2}\cdot\mathrm{E}_0\cdot\varepsilon^2 \tag{10}$$

Such a variable can be used to obtain a thermodynamically based damage criterion:

$$\mathcal{Y}(\mathrm{D},\varepsilon) - \mathcal{Y}_{crit}(\mathrm{D}) \leq 0 \tag{11}$$

Where $\mathcal{Y}_{crit}$ is the critical damage energy release. Due to different values of the parameters of Eq. (9), it can be necessary to introduce the dependency on D parameter into $\mathcal{Y}_{crit}$ in Eq. (11). We will see in the following that it is possible to obtain the same strain-stress behavior (as shown in Fig. 3) from two distinct damage models.

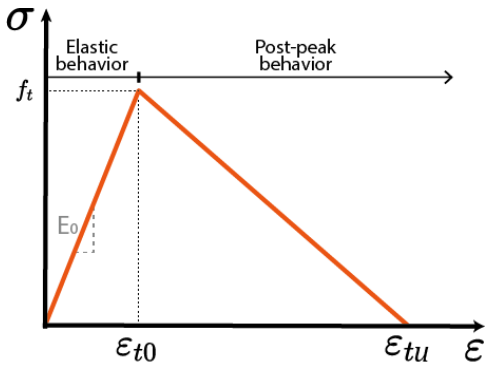

Figure 3: Strain-stress curve that can be obtained from two different damage constitutive models given by Eq. (12a) and Eq. (12b)

They are constructed using some particular values of α and β and if the equivalent condition in Eq. (11) is satisfied, the critical damage energy release can be obtained by simple algebra in the form of Eq.

(12a), and Eq. (12b):

$$1^{st}\text{ model}\begin{cases}\alpha = 1\\ \beta = 0\end{cases} \qquad \mathcal{Y}_{crit}(\mathrm{D}) = \frac{\mathrm{E}_0}{2\left(\frac{1}{\varepsilon_{t0}}+\mathrm{D}(\frac{1}{\varepsilon_{tu}}-\frac{1}{\varepsilon_{t0}})\right)^2} \tag{12a}$$

$$2^{nd}\text{ model}\begin{cases}\alpha = 1\\ \beta = \frac{\varepsilon_{tu}}{\varepsilon_{t0}} - 1\end{cases} \qquad \mathcal{Y}_{crit} = \frac{\mathrm{E}_0\cdot\varepsilon_{t0}\cdot\varepsilon_{tu}}{2} \tag{12b}$$

Moreover, Table 1 resumes the simulation parameters as proposed by Vignjevic *et al.* [6]:

Parameter	**Sign**	**Value**
Young modulus	E_0	$70.8\ [GPa]$
Volumetric mass density	ρ	$1550\ [kg/m^3]$
Initial failure strain	ε_{t0}	$0.022\ [-]$
Critical failure strain	ε_{tu}	$0.060\ [-]$
Displacement velocity	c	$7.0\ [m/s]$

Table 1: Input data for dynamic simulation of strain-softening bar

3 Results

We first aim at validating the use of a standard SPH formulation with the normalization of the kernel function and its corrected derivative form. For this purpose, the case study proposed by Vignjevic *et al.* [6] was reproduced in order to demonstrate the mesh independency. For this simulation, h-size is equal to 2.5 (Eq. 4) for three different particle densities (number of longitudinal particles: 101, 151, and 201). In all simulations, we use the damage model composed of Eq. (12a). Also, the resulting profiles are calculated as means of 5 nearest neighbors values.

Fig. 4 first presents the results for the longitudinal profile of the damage variable D simulated by Vignjevic *et al.* (a) and by the present study (b). It can be observed that the size of the damage zone does not depend on the density of the particles, which confirms the absence of mesh dependence. What is more, SPH results present a smoothed pic of damage variable instead of the $0-1$ discontinuity obtained with local methods. Another observation concerns the peak values obtained in each configuration. In the reference results, these values are non-monotonous concerning the number of particles. In the present simulations, the damage peak value increases with the increase of particle density and seems to converge toward the value of 0.28 for the densest configuration.

The second line of graphics in Fig. 4 represents the strain rate longitudinal profile. It shows that our formulation presents an oscillatory aspect absent from the reference result. Nevertheless, qualitatively, the present result (d) is coherent with the reference one (c) as well as the analytical solution proposed by Bažant and Belytschko [3].

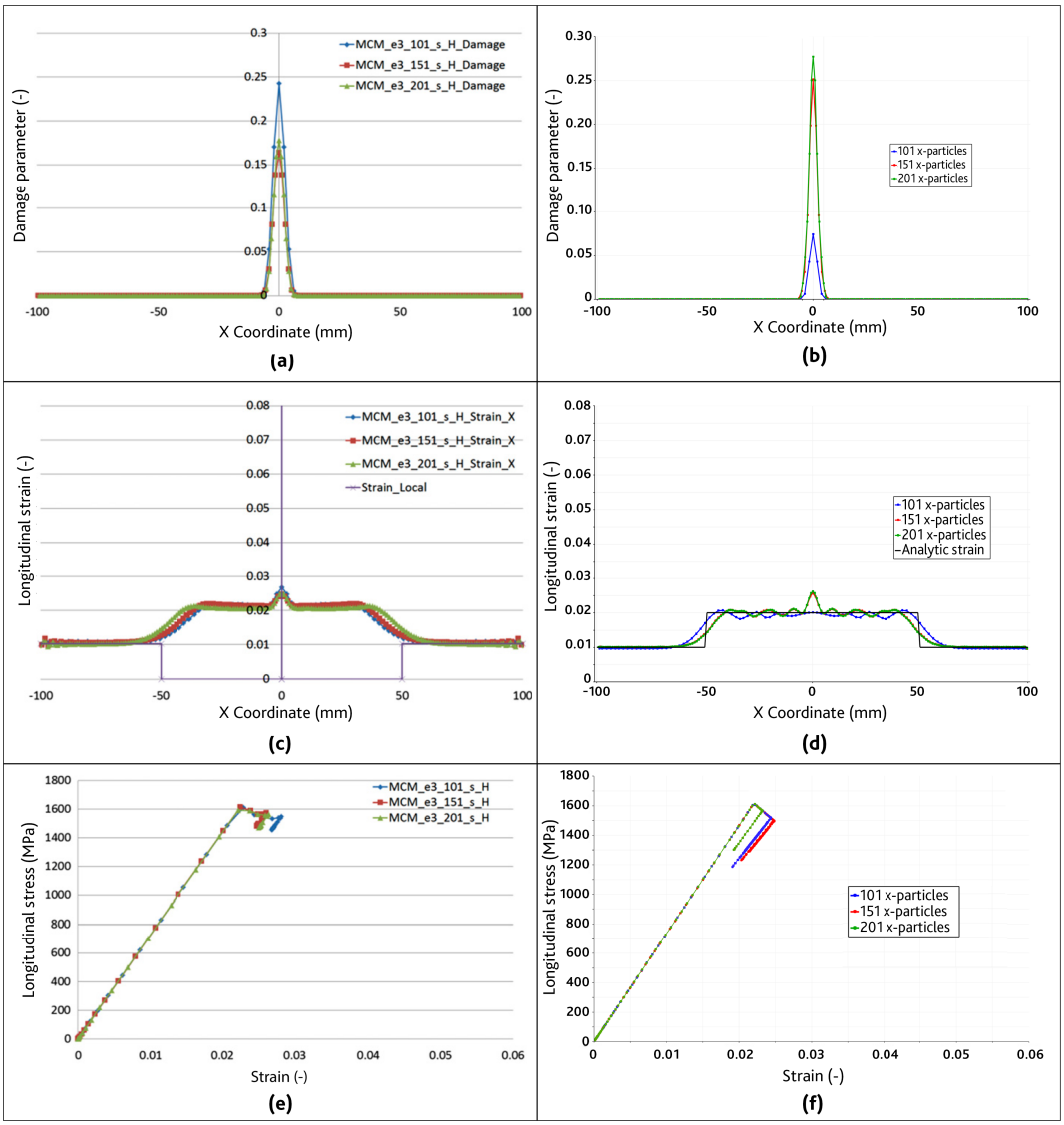

Figure 4: Total Lagrangian SPH [6] (left) and normalized-corrected SPH (right) model validation following damage (a,b), strain (c,d) and strain-stress (e,f) behavior for different particle densities and following damage model from Eq. (12a)

In the rest of Fig. 4, the relationship between the strain rate and the 1st Piola-Kirchhoff stress is presented for the reference (e) and the present model (f). It was calculated for the particle located at the center of the bar, such particle choice is justified due to the dynamic nature of the phenomenon. With this representation, we confirm the absence of mesh dependence on post-peak behavior. It can be seen, that the corrected and normalized SPH formulation presents a linear behavior that follows precisely the underlying constitutive law.

Another analysis proposed by Vignjevic *et al.* was to study the influence of three different values of the numerical parameter h-length (as presented in Eq. 4) for the same bar configuration of 201 longitudinal particles. The results of the present formulation, illustrated in Fig. 5, show that the size of the damaged zone is related to such numerical parameter (several studies present this parameter as a characteristic length of the material).

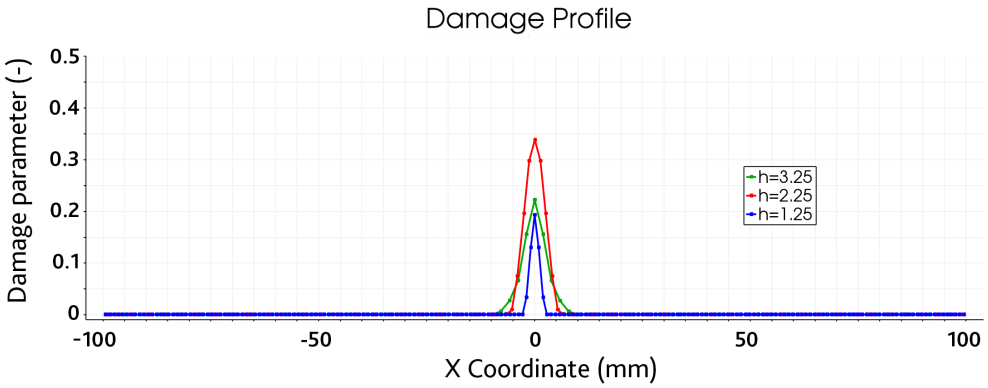

Figure 5: Damage parameter D longitudinal profile for h=1.25, h=2.25 and h=3.25 and its influence on the damage zone size following damage model from Eq. (12a)

Moreover, in order to verify the influence of damage model formulation on the overall behavior of the system, the same bi-traction simulations are performed with both models (Eq. 12b and Eq. 12a) and compared in Fig. 6. Despite different damage formulations, both models result in the same strain-stress constitutive law. Observing the longitudinal profile of the damage variable D (a), the second model shows lower peak values but stays monotonous and converges with increasing particle density. Also, the longitudinal profiles of displacement (b), strain (c) and 1st Piola-Kirchhoff stress (d) show that the differences between both damage models are no longer visible. Thus, we can conclude that the introduction of a new damage formulation only influenced the damaged zone, while keeping the same behavior of the other parts of the system.

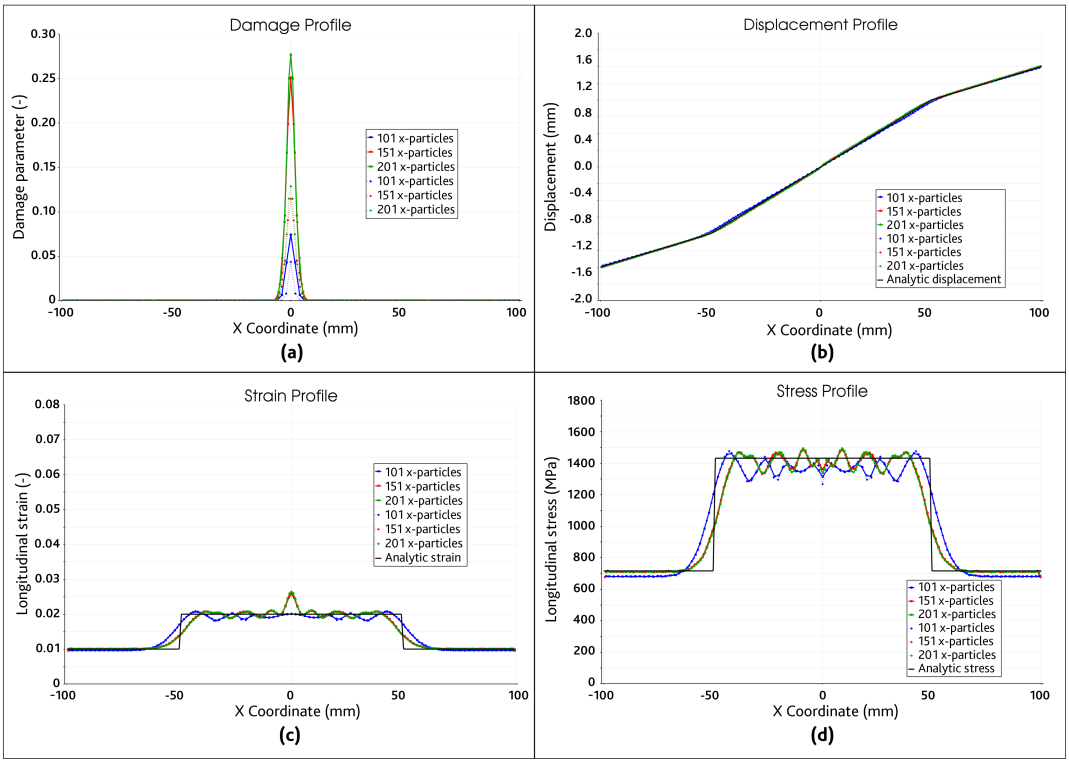

Figure 6: Longitudinal bar profile of damage (a), displacement (b), strain (c) and stress (d) for the energy-based damage models from Eq. (12a) (solid lines) and Eq. (12b) (dotted lines) for different particle densities.

4 Concluding remarks

This study aims to enhance the understanding of the mechanical behavior of damageable elastic solid material, an essential component of the coupled hydromechanical phenomena needed to model the partially saturated clay rocks. The computations were carried out using a non-local particulate Lagrangian model (Smoothed Particles Hydrodynamics), where a normalized-corrected formulation was validated with simulations of a strain-softening bar under tensile stress. Furthermore, the obtained results show that the proposed model can capture both damage growth and localization in dynamic conditions. The non-local computing method results in a no-mesh size dependency of the damage length zone, overtaking the ill-posedness of the underlying mathematical problem. However, this size is related to the SPH numerical parameter, which defines the size of the smoothing/averaging neighborhood.

Two different energy-based models, with different formulations but providing the same strain-stress curve, were simulated. It has been shown that the introduction of different damage formulation influenced only the results inside the damaged zone. This methodological study will be helpful to guide the application of the SPH method to partially or entirely saturated natural rocks.

Acknowledgements

This research has received financial support from the French National Research Agency (ANR) through the HydroGeoDam project under grant no. ANR-17-CE06-0016.

References

[1] P. Marschall, S. Horseman, and T. Gimmi. Characterisation of gas transport properties of the Opalinus Clay, a potential host rock formation for radioactive waste disposal. *Oil and Gas Science and Technology*, 60(1):121–139, 2005.

[2] Robert Cuss, Jon Harrington, Richard Giot, and Christophe Auvray. Experimental observations of mechanical dilation at the onset of gas flow in Callovo-Oxfordian claystone. *Clays in Natural and Engineered Barriers for Radioactive Waste Confinament. Geological Society, London, Special Publications*, 400(iii):507–519, 2014.

[3] Zdeněk P Bažant and Ted B Belytschko. Wave propagation in a strain-softening bar: exact solution. *Journal of Engineering Mechanics*, 111(3):381–389, 1985.

[4] Zdeněk P Bažant. Why continuum damage is nonlocal: justification by quasiperiodic microcrack array. *Mechanics Research Communications*, 14(5-6):407–419, 1987.

[5] Zdeněk P Bažant. Why continuum damage is nonlocal: Micromechanics arguments. *Journal of Engineering Mechanics*, 117(5):1070–1087, 1991.

[6] R Vignjevic, N Djordjevic, S Gemkow, T De Vuyst, and J Campbell. Sph as a nonlocal regularisation method: Solution for instabilities due to strain-softening. *Computer Methods in Applied Mechanics and Engineering*, 277:281–304, 2014.

[7] Robert A Gingold and Joseph J Monaghan. Smoothed particle hydrodynamics: theory and application to non-spherical stars. *Monthly notices of the royal astronomical society*, 181(3):375–389, 1977.

[8] L. B. Lucy. A numerical approach to the testing of the fission hypothesis. , 82:1013–1024, December 1977.

[9] M. B. Liu and G. R. Liu. Meshfree particle simulation of micro channel flows with surface tension. *Computational Mechanics*, 2005.

[10] Damien Violeau and R. Issa. Numerical modelling of complex turbulent free-surface flows with the SPH method: An overview, 2007.

[11] J. J. Monaghan and A. Kocharyan. SPH simulation of multi-phase flow. *Computer Physics Communications*, 1995.

[12] A. M. Tartakovsky, N. Trask, K. Pan, B. Jones, W. Pan, and J. R. Williams. Smoothed particle hydrodynamics and its applications for multiphase flow and reactive transport in porous media. *Computational Geosciences*, 20(4):807–834, 2016.

[13] Larry D Libersky and Albert G Petschek. Smooth particle hydrodynamics with strength of materials. In *Advances in the free-Lagrange method including contributions on adaptive gridding and the smooth particle hydrodynamics method*, pages 248–257. Springer, 1991.

[14] Larry D. Libersky, Albert G. Petschek, Theodore C. Carney, Jim R. Hipp, and Firooz A. Allahdadi. High strain lagrangian hydrodynamics a three-dimensional SPH code for dynamic material response. *Journal of Computational Physics*, 1993.

[15] A.K. Chaniotis, D. Poulikakos, and P. Koumoutsakos. Remeshed Smoothed Particle Hydrodynamics for the Simulation of Viscous and Heat Conducting Flows. *Journal of Computational Physics*, 2002.

[16] M. B. Liu and G. R. Liu. Smoothed particle hydrodynamics (SPH): An overview and recent developments. *Archives of Computational Methods in Engineering*, 2010.

[17] Aliaksei Pazdniakou and Magdalena Dymitrowska. Migration of gas in water saturated clays by coupled hydraulic-mechanical model. *Geofluids*, 2018, 2018.

[18] Joseph J. Monaghan, Herbert E. Huppert, and M. Grae Worster. Solidification using smoothed particle hydrodynamics. *Journal of Computational Physics*, 2005.

[19] L Lobovskya and J Krena. Smoothed particle hydrodynamics modelling of fluids and solids. 2007.

[20] ANDRA. Dossier 2005 argile. évaluation de la faisabilité du stockage géologique en formation argileuse. Technical report, Agence Nationale pour la estion des Déchets Radioactifs, 2005.

[21] A.G. Corkum and C.D. Martin. The mechanical behaviour of weak mudstone (opalinus clay) at low stresses. *International Journal of Rock Mechanics and Mining Sciences*, 44(2):196 – 209, 2007.

[22] Luc Dormieux and Djimedo Kondo. Approche micromécanique du couplage perméabilité-endommagement. *Comptes Rendus Mécanique*, 332(2):135 – 140, 2004.

[23] Jean Lemaitre. A continuous damage mechanics model for ductile fracture. *Journal of engineering materials and technology*, 107(1):83–89, 1985.

[24] Jean Lemaitre and Jean-Louis Chaboche. *Mechanics of solid materials*. Cambridge university press, 1994.

[25] P. Ponte Castañeda and J.R. Willis. The effect of spatial distribution on the effective behavior of composite materials and cracked media. *Journal of the Mechanics and Physics of Solids*, 43(12):1919 – 1951, 1995.

[26] Luc Dormieux and Djimedo Kondo. *Micromechanics of fracture and damage*. John Wiley & Sons, 2016.